

Observation of Hot-Electron Energy Loss through the Emission of Phonon-Plasmon Coupled Modes in GaAs

C. L. Petersen and S. A. Lyon

Department of Electrical Engineering, Princeton University, Princeton, New Jersey 08544-5263

(Received 11 December 1989)

We have directly observed hot-electron energy loss through the emission of phonon-plasmon coupled modes in *n*-type Si-doped GaAs. The self-compensation of silicon in GaAs was exploited to allow observation of hot-electron recombination with neutral Si acceptors in a high background concentration of free electrons. We have obtained hot-luminescence data which exhibit a peak due to the initial unrelaxed hot electrons followed by a peak lower in energy by the L^+ coupled-mode energy. The lower-energy peak corresponds to hot-electron relaxation via emission of a phonon-plasmon coupled mode. The observed peak agrees well with energy-loss calculations.

PACS numbers: 72.10.Di, 71.45.Gm, 73.20.Mf

Hot carrier relaxation via phonon emission in semiconductors, especially GaAs and GaAs/AlGaAs heterostructures, has been well studied. In particular, the emission of longitudinal-optical (LO) phonons by extreme non-equilibrium electrons and by hot thermal distributions of electrons has been measured by a variety of steady-state (cw) and time-resolved techniques.¹⁻¹¹ Attention has recently turned towards understanding the thermalization of hot electrons in the presence of a sea of cold electrons¹²⁻¹⁴ where, analogous to metals, the collective (plasmon) modes should play a major role in the energy-relaxation process.

In GaAs the LO phonons mix with the plasmons and hence energy loss through emission of phonon-plasmon coupled modes is expected. Coupled modes are well documented in GaAs and were first observed experimentally using Raman scattering.¹⁵ Surface-plasmon emission has been seen in tunneling experiments,¹⁶ but evidence for plasmon emission by energetic carriers in semiconductors has thus far been indirect. Phonon-plasmon coupled modes have been invoked to explain hot-electron cooling in two-dimensional structures.^{17,18} Coupled modes have also been suggested as the primary energy-loss mechanism of ballistically injected carriers in hot-electron transistors and may be the reason the devices have often not met expectations.¹⁹⁻²¹

We report the direct observation of hot-electron energy loss to phonon-plasmon coupled modes in *n*-type GaAs. Coupled-mode emission is found to dominate the initial energy loss of 280-meV electrons injected into a background electron density of $n \sim 7 \times 10^{17} \text{ cm}^{-3}$. At lower electron densities ($3 \times 10^{16} \text{ cm}^{-3}$), LO phonon scattering still dominates and coupled-mode emission is not seen. Our experimental observations are in good agreement with a calculation including both phonons and a Lindhard dielectric function for the electron gas.

The present experiments are based upon the technique of Dymnikov,⁴ Mirlin *et al.*,⁵ and Zakharchenya *et al.*⁶ where hot electrons are optically injected into *p*-type GaAs held at liquid-helium temperatures. At these temperatures the acceptors are largely neutral and provide a well-defined energy for holes which can then radiatively

recombine with energetic electrons. Since the highest-energy peak of the luminescence is offset from the excitation energy by the sum of both the neutral acceptor energy and the kinetic energy of the hole created in the absorption process, the hot luminescence can be unambiguously separated from Raman scattering and other signals.²² Relaxation rates due to LO phonon emission and intervalley scattering have been obtained by measuring the depolarization of the hot luminescence in a magnetic field.^{4,5} Ulbrich, Kash, and Tsang²³ have also used this hot luminescence (without the magnetic field) to measure intervalley scattering times, while Fasol and Hughes²⁴ have used the technique to investigate the valence-band structure of GaAs.

A typical spectra obtained from a Be-doped ($p \sim 1.1 \times 10^{17} \text{ cm}^{-3}$) sample is shown as the upper curve in Fig. 1. The highest-energy peak (at 1.85 eV) corresponds to

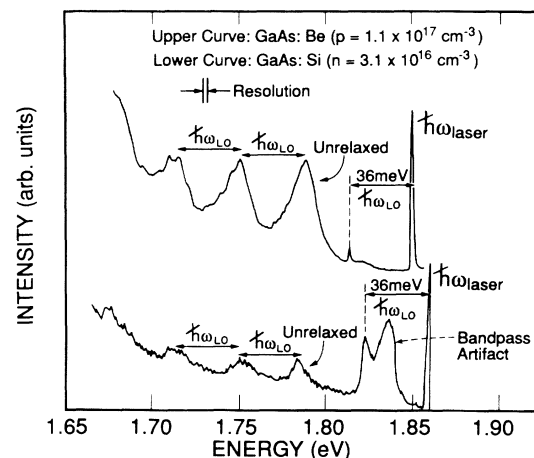


FIG. 1. Luminescence spectra of hot electrons recombining with neutral acceptors in GaAs. The upper curve depicts a spectrum from a Be-doped ($p = 1.1 \times 10^{17} \text{ cm}^{-3}$) sample. The lower curve was obtained from a Si-doped sample with an electron concentration of $3.1 \times 10^{16} \text{ cm}^{-3}$. The intensity scales and zeros are different in each case. The two-stage spectrometer used produces artifacts at the laser energy and short-wavelength bandpass cutoff (see text).

the dye laser wavelength and is an artifact of the two-stage (a bandpass filter stage followed by a single spectrograph stage) spectrometer used in these experiments. Below the laser energy by 36 meV is a small peak due to Raman scattering, and below this is a larger peak which corresponds to the initial (unrelaxed) hot electrons recombining with neutral acceptors. Following the unrelaxed peak is a series of lower-energy peaks separated by one LO phonon energy which arises from those electrons that have relaxed via successive LO phonon emission before recombining with neutral acceptors. These peaks are typically many orders of magnitude (~ 6 - 9) weaker in intensity than the band-gap signal, primarily because phonon emission is much faster than the radiative recombination. The lower curve in Fig. 1 was obtained in a Si-doped sample with $n \sim 3 \times 10^{16} \text{ cm}^{-3}$. Here we have used the fact that silicon is incorporated into GaAs as both donor and acceptor, donors being predominant for our samples. This allows us to study the hot-electron-neutral-acceptor recombination in the presence of a Fermi sea of electrons. As in the upper curve, the highest-energy feature (at 1.858 eV) corresponds to the dye laser wavelength. Visible also is a second artifact of the spectrometer (at 1.837 eV) which is only apparent at low signal intensities and is caused by the short-wavelength cutoff of the bandpass stage. Below the bandpass artifact are the peaks due to Raman scattering and the hot-electron photoluminescence, similar to the upper curve. The hot luminescence is much weaker in n -type GaAs than in p -type GaAs mainly because only a very small fraction of the Si acceptors are neutral. In addition, the peak-to-background ratio of the hot luminescence in GaAs:Si is less than GaAs:Be which has been interpreted as implying that electron-electron scattering is becoming important even at this low electron density¹³ (note that the absolute intensity scales and zeros are different for each case). Recent experiments¹² (using relatively hot plasmas) have quantified this more precisely and suggest that the rates of energy loss to electrons and LO phonons become equal at a plasma density of about $8 \times 10^{16} \text{ cm}^{-3}$.

The nature of the hot luminescence in n -type samples differs in several important respects from that in the p -type case. First, since the only holes available for trapping on acceptor sites are photogenerated, the luminescence intensity depends on the square of the incident intensity rather than the simple linear dependence in p -type materials. However, the incident intensity cannot be increased without bound since the injected carriers heat the electron gas which causes the high-energy tail of the band-gap luminescence to increase, obscuring the hot-luminescence signal. The incident laser photon energy can be increased to avoid the high-energy tail, but another limit becomes manifest near the energy at which holes can be excited from the split-off band ($\sim 1.86 \text{ eV}$ in GaAs). At this laser wavelength, recombination with hot holes in the split-off band and resonantly enhanced

second-order Raman scattering dominate the hot luminescence. We found that excitation energies between 1.83 and 1.86 eV were optimal.

The doping concentration must also be carefully chosen in order to observe phonon-plasmon coupled-mode emission. There should be enough free electrons present so that the coupled-mode energy is clearly distinguishable from the LO phonon energy; because of broadening arising from valence-band warping this requires a shift of $\sim 5 \text{ meV}$ or more in our experiments. Too large a shift, however, would again push the hot-luminescence signal into the high-energy tail of the band-gap signal. A charge-coupled device array detector was utilized in conjunction with a high-throughput spectrometer in order to detect the weak hot-luminescence signal.

The data obtained from a sample with $n \sim 7 \times 10^{17} \text{ cm}^{-3}$ excited by the 676.4-nm line (1.833 eV) from a Kr^+ laser are shown as the upper curve in Fig. 2. As before, the two highest-energy features are artifacts and correspond to the laser energy and bandpass cutoff, respectively. Below these artifacts are peaks due to Raman processes. The two main Raman peaks are labeled in Fig. 2 and correspond to LO phonons within the surface depletion region and the L^+ phonon-plasmon coupled mode arising from the bulk region. Slightly higher in energy than the LO modes are two small features (not labeled) corresponding to a weak, forbidden, transverse-optical (TO) phonon and the L^- mode.

Below the Raman lines is a peak at 1.762 eV due to

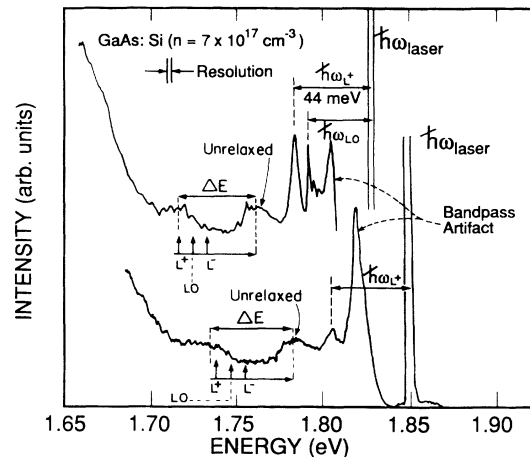


FIG. 2. Hot-luminescence spectra obtained from a Si-doped sample with a carrier concentration of $7 \times 10^{17} \text{ cm}^{-3}$. The upper curve was obtained using the 676.4-nm line (1.833 eV) of a Kr^+ laser. Peaks due to Raman scattering and the spectrometer artifacts are indicated. The unrelaxed hot-electron peak is at 1.762 eV and ΔE below this is a peak due to scattered hot electrons at 1.718 eV. The relevant scattering energies (L^+ , LO, L^-) are indicated on the horizontal axis just below the unrelaxed peak (see text). The lower curve was obtained using a dye laser operating at 1.852 eV, and it can be seen that the hot-luminescence peaks track with the laser.

unrelaxed hot electrons recombining with neutral acceptors. A broad, weak feature ΔE (~ 44 meV) below the unrelaxed peak is seen at 1.718 eV. Further peaks cannot be resolved due to the rapidly increasing band-gap signal.

To ensure that the peak at 1.718 eV is associated with the scattered hot electrons and not an extraneous signal coincidentally at the expected energy, we varied the incident laser wavelength. True hot luminescence should move with the laser. An Ar⁺ pumped DCM (Ref. 25) dye laser operating in the range from 1.8 to 1.9 eV was used for the excitation. Data obtained using $\hbar\nu_{\text{laser}} = 1.85$ eV are shown as the lower curve of Fig. 2. It can be seen that both the unrelaxed peak and the 1.718-eV feature shift with the laser energy. The separation between these peaks, ΔE (~ 46 meV in this case), is equivalent to ΔE obtained from the upper curve to within the experimental uncertainty.

The origin of this new peak can be understood by evaluating the energy and wave-vector-dependent scattering rate. Since the initial electron kinetic energy is an order of magnitude larger than either the Fermi energy or the experimentally accessible scattering energies, only single scattering is considered. The differential scattering rate $dR(\omega)$ is given by^{26,27}

$$dR(\omega) = \frac{2e^2 m_e^*}{\pi \hbar^2 k_i} d\omega \int_{k_i - k_f}^{k_i + k_f} \text{Im} \left[\frac{-1}{\epsilon(q, \omega)} \right] \frac{dq}{q}, \quad (1)$$

where \mathbf{q} is the wave-vector transfer between the initial wave vector \mathbf{k}_i and the final wave vector \mathbf{k}_f , m_e^* is the electron effective mass, e is the electronic charge, and $\hbar\omega$ is the scattered energy loss. The dielectric function $\epsilon(q, \omega)$ contains contributions from both phonons and electrons,

$$\epsilon(q, \omega) = \epsilon_\infty \frac{\omega^2 - (\omega_{\text{LO}} + i/\tau)^2}{\omega^2 - (\omega_{\text{TO}} + i/\tau)^2} + \chi_e(q, \omega), \quad (2)$$

where ω_{LO} and ω_{TO} are the respective phonon frequencies, and the complex quantity i/τ has been added to give the experimentally observed exponential time decay with a lifetime of 7 ps.²⁸ The noninteracting Lindhard (random phase approximation) form of $\chi_e(q, \omega)$ is applicable since we have a weakly coupled plasma, and is given by²⁶

$$\chi_e(q, \omega) = \beta \left\{ \left[1 - \frac{1}{4} \left(\frac{y}{x} + x \right)^2 \right] \ln \left[\frac{y+x(x+2)}{y+x(x-2)} \right] + \left[1 - \frac{1}{4} \left(x - \frac{y}{x} \right)^2 \right] \ln \left[\frac{y-x(x+2)}{y-x(x-2)} \right] \right\}, \quad (3)$$

where $\beta = m_e^* e^2 k_f / \pi \hbar^2 q^2$, $x = q/k_F$, and $y = \hbar\omega/E_F$, where k_F and E_F are the Fermi wave vector and energy, respectively.

The integral in (1) has been evaluated by integrating

over the final density of states consistent with momentum and energy conservation within the effective-mass approximation. To account for the broadening of the initial (unrelaxed) energy distribution caused by valence-band anisotropy in the real crystal structure, a Gaussian distribution of unrelaxed electrons with a full width at half maximum of 12 meV (the observed value of the unrelaxed peak) was used in the calculations. The resulting energy-dependent scattering rate for a free-electron density of $n \sim 7 \times 10^{17} \text{ cm}^{-3}$ and laser excitation energy of 1.833 eV is shown in Fig. 3. The contribution from each of the individual scattering mechanisms is also shown, and it can be clearly seen that the L^+ plasmon-phonon coupled mode is the dominant energy-loss mechanism while the L^- and LO phonon modes contribute only a weak low-energy tail to the scattered distribution of electrons. The LO phonon mode exists only at long wave vector (where the scattering is sharply reduced due to the Coulombic interaction) since the coupled modes are strongly damped in the region where single-pair excitations are allowed (inset of Fig. 3). From the Raman scattering we obtain the L^+ coupled-mode energy (44 meV), the LO phonon energy (36 meV), and also the L^- energy (30 meV). These energies are indicated relative to the unrelaxed peak on Fig. 2, and it can be seen that ΔE corresponds to the L^+ -mode energy. This leads us to conclude that the low-energy peak arises from hot electrons that have relaxed via emission of a phonon-plasmon coupled mode.

The magnitudes of the peak heights provide a good estimate of the scattering rates although obtaining precise, quantitative results is difficult in the present experiments. Based on the relatively low intensity of the observed

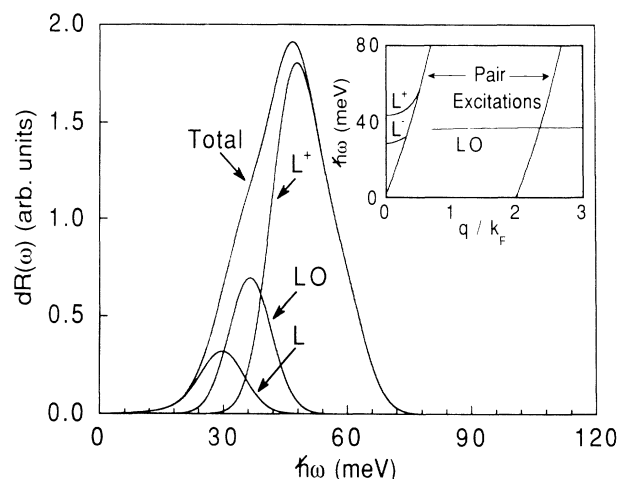


FIG. 3. The differential scattering rate $dR(\omega)$, calculated for $n = 7 \times 10^{17} \text{ cm}^{-3}$ and $\hbar\nu_{\text{laser}} = 1.833$ eV, is shown. The initial electron distribution was taken as Gaussian with a full width at half maximum of 12 meV (see text). The individual contributions to the scattering from the L^- , LO, and the L^+ modes are indicated. Inset: Dispersion of all three modes.

peaks, we would expect that coupled-mode scattering in our energy and density regime is at least as fast as scattering due to LO phonons in undoped GaAs which has been measured to be in the range of 100–200 fs.^{2,29,30} The total scattering rate, given an initial electron energy of 280 meV and $n=7\times 10^{17}$ cm⁻³, has been calculated to be nearly 3 times that of undoped GaAs. Using a scattering time of ~ 35 fs and an electron velocity of 1.2×10^8 cm/s, a mean free path of ~ 400 Å is found. This is in good agreement with a previous, independent, determination¹³ of the inelastic-scattering length of ~ 380 Å (for $n=7\times 10^{17}$ cm⁻³) in the same sample.

In summary, we have used cw photoluminescence to study the relaxation of highly nonequilibrium electrons in *n*-type GaAs. In lightly doped samples ($n\sim 3\times 10^{16}$ cm⁻³) we find that the luminescence peaks characteristic of hot-electron relaxation via LO phonon emission are reduced in magnitude indicating that electron-electron scattering is becoming important. At higher electron densities ($n\sim 7\times 10^{17}$ cm⁻³) we find a luminescence peak due to relaxation by the emission of a phonon-plasmon coupled mode. The width and energy of the luminescence peak is in good agreement with calculations of the scattering.

This work was supported in part by grants from Bellcore, General Motors, and the National Science Foundation through the Presidential Young Investigator Program under Grant No. ECS-8351620. The authors are associated with the Advanced Technology Center for Photonics and Opto-electronic Materials established at Princeton University by the State of New Jersey.

¹Jagdeep Shah and R. C. C. Leite, Phys. Rev. Lett. **22**, 1304 (1969).

²R. G. Ulbrich, Phys. Rev. B **8**, 5719 (1973).

³C. V. Shank, R. L. Fork, R. F. Leheny, and Jagdeep Shah, Phys. Rev. Lett. **42**, 112 (1979).

⁴V. D. Dymnikov, Zh. Eksp. Teor. Fiz **77**, 1107 (1979) [Sov. Phys. JETP **50**, 559 (1979)].

⁵D. N. Mirlin, I. Ya. Karlik, L. P. Nikitin, I. I. Reshina, and V. F. Sapega, Solid State Commun. **37**, 757 (1980).

⁶B. P. Zakharchenya, D. N. Mirlin, V. I. Perel', and I. I. Reshina, Usp. Fiz. Nauk **136**, 459 (1982) [Sov. Phys. Usp. **25**, 143 (1982)].

⁷C. L. Tang and D. J. Erskine, Phys. Rev. Lett. **51**, 840

(1983).

⁸J. F. Ryan, R. A. Taylor, A. J. Turberfield, Angela Maciel, J. M. Worlock, A. C. Gossard, and W. Wiegmann, Phys. Rev. Lett. **53**, 1841 (1984).

⁹Kathleen Kash, Jagdeep Shah, Dominique Block, A. C. Gossard, and W. Wiegmann, Physica (Amsterdam) **134B**, 189 (1985).

¹⁰C. H. Yang, Jean M. Carlson-Swindle, S. A. Lyon, and J. M. Worlock, Phys. Rev. Lett. **55**, 2 (1985).

¹¹C. L. Petersen and S. A. Lyon, Phys. Rev. Lett. **63**, 2849 (1989).

¹²J. A. Kash, Phys. Rev. B **40**, 3455 (1989).

¹³S. A. Lyon and C. L. Petersen, in *Ultrafast Laser Probe Phenomena in Bulk and Microstructure Semiconductors II*, edited by Robert R. Alfano, SPIE Conference Proceedings No. 942 (International Society for Optical Engineering, Bellingham, WA, 1988), p. 264.

¹⁴W. H. Knox, D. S. Chemla, G. Livescu, J. E. Cunningham, and J. E. Henry, Phys. Rev. Lett. **61**, 1290 (1988).

¹⁵A. Mooradian and G. B. Wright, Phys. Rev. Lett. **16**, 999 (1966).

¹⁶D. C. Tsui, Phys. Rev. Lett. **22**, 293 (1969).

¹⁷C. H. Yang and S. A. Lyon, Physica (Amsterdam) **134B**, 309 (1985).

¹⁸J. K. Jain, R. Jalabert, and S. Das Sarma, Phys. Rev. Lett. **60**, 353 (1988).

¹⁹M. A. Hollis, S. C. Palmeter, L. F. Eastman, H. V. Dandekar, and P. M. Smith, IEEE Electron Dev. Lett. **4**, 440 (1983).

²⁰A. F. J. Levi, J. R. Hayes, P. M. Platzman, and W. Wiegmann, Phys. Rev. Lett. **55**, 2071 (1985).

²¹P. Lugli and D. K. Ferry, IEEE Electron Dev. Lett. **6**, 25 (1985).

²²G. Fasol, K. Ploog, and E. Bauser, Solid State Commun. **54**, 383 (1985).

²³R. G. Ulbrich, J. A. Kash, and J. C. Tsang, Phys. Rev. Lett. **62**, 949 (1989).

²⁴G. Fasol and H. P. Hughes, Phys. Rev. B **33**, 2953 (1986).

²⁵DCM stands for 4-(dicyanomethylene)-2-methyl-6-(*p*-dimethyl-amino-styryl)-4H-pyran.

²⁶P. M. Platzman and P. A. Wolffe, in *Waves and Interactions in Solid State Plasmas*, Solid State Physics Supplement 13, edited by H. Ehrenreich, F. Seitz, and D. Turnbull (Academic, New York, 1973).

²⁷P. Nozieres and D. Pines, Nuovo Cimento **9**, 470 (1958).

²⁸D. von der Linde, J. Kuhl, and H. Klingenberg, Phys. Rev. Lett. **44**, 1505 (1980).

²⁹J. A. Kash, J. C. Tsang, and J. M. Hvam, Phys. Rev. Lett. **54**, 2151 (1985).

³⁰G. Fasol, W. Hackenberg, H. P. Hughes, K. Ploog, E. Bauser, and H. Kano, Phys. Rev. B **41**, 1461 (1990).